

Levitation of Bose-Einstein condensates induced by macroscopic non-adiabatic quantum tunneling

Katsuhiro Nakamura* and Akihisa Kohi

Department of Applied Physics, Osaka City University, Osaka 558-8585, Japan

Hisatsugu Yamasaki

Department of Physics, Waseda University, Tokyo 169-8555, Japan

Víctor M. Pérez-García†

Departamento de Matemáticas, E. T. S. Ingenieros Industriales, Universidad de Castilla-La Mancha, 13071 Ciudad Real, Spain.

(Dated: February 6, 2008)

We study the dynamics of two-component Bose-Einstein condensates trapped in different vertical positions in the presence of an oscillating magnetic field. It is shown here how tuning appropriately the oscillation frequency of the magnetic field leads to the levitation of the system against gravity. This phenomenon is a manifestation of a macroscopic non-adiabatic tunneling in a system with internal degrees of freedom.

PACS numbers: 03.75.Lm, 03.75.Mn

The now classical observation of Bose-Einstein condensation with dilute atomic vapors in a series of experiments [1] has been the stimulus of a great number of experimental and theoretical works in the field of matter waves and macroscopic quantum dynamics.

Shortly after the production of single-component Bose-Einstein condensates (BECs), multicomponent condensates were observed [2, 3] in mixtures of two hyperfine states of ^{87}Rb , $|F = 1, m_f = -1\rangle$ and $|F = 2, m_f = 1\rangle$ with and without “sag” corresponding to equal or different trap centers, respectively. These works, together with other experiments which followed soon [4, 5, 6] stimulated many studies on multi-component BECs which open scenarios different from those found in single component BECs, for instance for their ground state and excitations.

In spinor BECs it is easy to induce Rabi-type transitions optically. Similar phenomena involving coupling of different states occur in tunneling of BECs in optical lattices or double-well potentials [6, 7, 8, 9, 10, 11, 12, 13, 14].

In this paper we describe a striking levitation phenomenon which occurs when both the spatial aspects of the dynamics are put together with the two internal degrees of freedom present in a two-component Bose-Einstein condensate in which transitions between components are driven by an oscillating magnetic field. In this scenario the dynamics splits into a fast complex spatio-temporal oscillation of the condensate wavefunctions together with a slow dynamical levitation of the total center of mass against gravity with neither applied mechanical force nor associated classical trajectories.

In this paper we will study the dynamics of two-component BECs where each component is trapped in different vertical positions as schematically indicated in

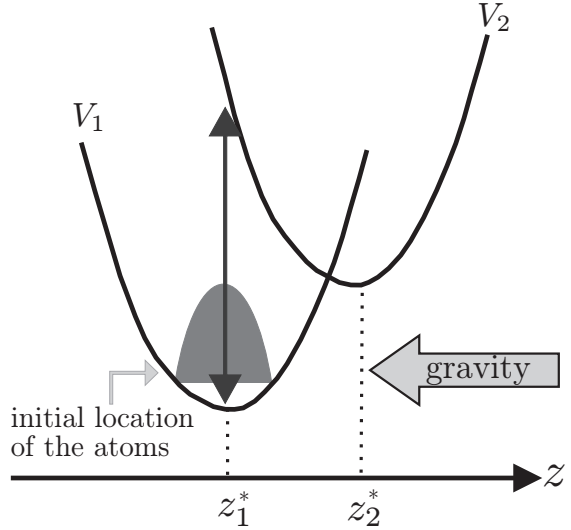


FIG. 1: Schematic plot of the setup studied in this paper. Each of the components of a two-component BEC is subject to the action of gravity and different confining potentials V_1 and V_2 with minima z_1^* and z_2^* , respectively. An oscillating magnetic field induces transitions between both states. A Franck-Condon type vertical transition is indicated by the black arrow. Initially all atoms are in the first component.

Fig. 1. An optical dipole trap together with a magnetic field gradient can provide such kind of confinement [10, 11]. To fix ideas we will consider our system to be the $|F = 1, m_f = -1\rangle$ and $|F = 2, m_f = 1\rangle$ hyperfine states of ^{87}Rb coupled by an oscillating magnetic field of frequency Ω inducing transitions between them. We shall pay a special attention to the situation of the Franck-Condon-type vertical transition [14, 15] shown in Fig.1. To simplify the treatment yet preserving the spatial aspects of the dynamics we will assume our system to be

magnetically tightly confined along one of the transverse directions [16] to two effective dimensions.

The Hamiltonian density of our system is

$$\mathcal{H} = \sum_{j=1}^2 \left(\frac{\hbar^2}{2m} |\nabla \psi_j|^2 + V_j |\psi_j|^2 + \frac{U_{jj}}{2} |\psi_j|^4 \right) + U_{12} |\psi_1|^2 |\psi_2|^2 + B \cos(\Omega t) (\psi_1^* \psi_2 + \psi_2^* \psi_1), \quad (1)$$

where V_j are the confining potentials acting on each of the species given by

$$V_j(x, z) = \frac{1}{2} m \omega^2 [x^2 + (z - z_j)^2] + \epsilon_j + mgz, \quad (2)$$

where ϵ_j stands for the internal electronic energy and g is the gravity constant. $V_j(x, z)$ has the minimum value $mz_j g - \frac{m}{2}(\frac{g}{\omega})^2 + \epsilon_j$ at $(x, z) = (0, z_j^* = z_j - g/\omega^2)$. U_{11}, U_{22} and $U_{12} = U_{21}$ are the effective nonlinear interaction coefficients defined by $U_{ij} = 4\pi\hbar^2 a_{ij} N/m\ell$ in 2-dimensional (2D) space where N is the total number of atoms and a_{ij} are the scattering lengths for binary collisions. Finally, $\ell = \sqrt{\hbar/m\omega}$ is a characteristic length.

The Gross-Pitaevskii equation (GPE) for the mean field dynamics of our system is derived through Lagrange equations with use of the Hamiltonian $H = \iint \mathcal{H} dx dz$. Additionally, we change to new variables scaled as $\omega t \rightarrow t$, $x/\ell \rightarrow x$, $z/\ell \rightarrow z$, $\ell\psi \rightarrow \psi$ and obtain

$$i \frac{\partial \psi_1}{\partial t} = \left[-\frac{1}{2} \nabla^2 + V'_1 + U'_{11} |\psi_1|^2 + U'_{12} |\psi_2|^2 \right] \psi_1 + B' \cos(\Omega' t) \psi_2 \quad (3a)$$

$$i \frac{\partial \psi_2}{\partial t} = \left[-\frac{1}{2} \nabla^2 + V'_2 + U'_{22} |\psi_2|^2 + U'_{21} |\psi_1|^2 \right] \psi_2 + B' \cos(\Omega' t) \psi_1 \quad (3b)$$

where $V'_j \equiv V'_j(x, z) = \frac{1}{2}[x^2 + (z - z_j)^2] + g'z + \epsilon'_j$ with $U'_{ij} = 4\pi N a_{ij} / \ell$, $B' = B/\hbar\omega$, $\Omega' = \Omega/\hbar\omega$, $g' = g/\ell\omega^2$ and $\epsilon'_j = \epsilon_j/\hbar\omega$ being dimensionless constants. The normalization condition for ψ is $\iint (|\psi_1|^2 + |\psi_2|^2) dx dz = 1$.

Initially we prepare a circularly-symmetric Gaussian wavepacket with its center of mass at $\mathbf{r}_1 = (0, z_1^*)$,

$$\psi_1 = \frac{1}{\sqrt{\pi} \left(1 + \frac{U'_{11}}{2\pi} \right)^{1/4}} \exp \left(-\frac{x^2 + (z - z_1^*)^2}{2\sqrt{1 + \frac{U'_{11}}{2\pi}}} \right) \quad (4)$$

which minimizes the energy $E = \int d^2 \mathbf{r} (\frac{1}{2} |\nabla \psi_1|^2 + V'_1 |\psi_1|^2 + \frac{U'_{11}}{2} |\psi_1|^4)$ over a family of gaussian functions and approximates the ground state when all atoms are in state $|1\rangle$. We then apply an external microwave field that induces a Franck-Condon type transition between the species with frequency $\Omega' = \Delta V'_{12} = V'_2(0, z_1^*) - V'_1(0, z_1^*)$. Without loss of generality, we will consider the case $z_2^* = -z_1^*$. After the oscillating magnetic field is switched on, we study the dynamics according to Eq. (3).

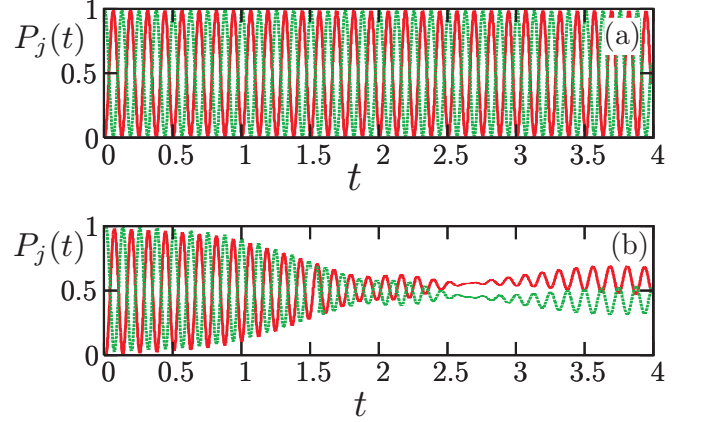


FIG. 2: [Color online] Time dependence of the population mixing for the case of resonance of Franck-Condon type. Dashed and solid lines stand for $P_1 = \iint |\psi_1|^2$ and $P_2 = \iint |\psi_2|^2$, respectively for $B' = 50$. (a) $\delta z = 1.0$ (b) $\delta z = 5.0$.

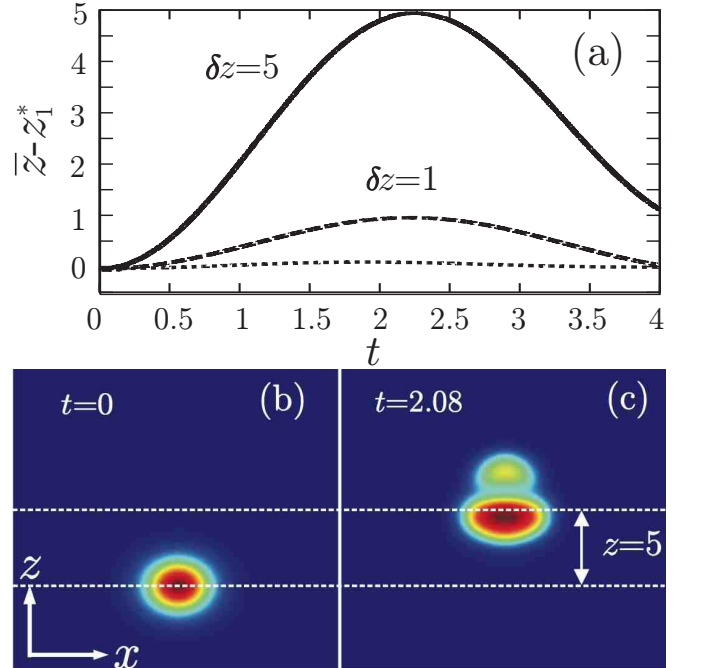


FIG. 3: (a) Time evolution of the center of mass $\bar{z} = \int \psi^\dagger z \psi d^2 \mathbf{r} = \int z (|\psi_1|^2 + |\psi_2|^2) d^2 \mathbf{r}$ for $B' = 50$ and $\delta z = 1.0$ (broken line) and $\delta z = 5.0$ (solid line). The dotted line stands for the case far from the standard resonance ($\Omega' = 1, \delta' = 500$) with $\delta z = 5$. (b) and (c) Pseudocolor plots of $|\Psi(x, z, t)|^2 = |\psi_1(x, z, t)|^2 + |\psi_2(x, z, t)|^2$ for $t = 0$ and $t = 2.08$ on the region $(x, z) \in [-6.5, 6.5] \times [-9.6, 9.6]$ showing the rising (white broken lines) of the total wavefunction.

Since our results are based on long-time numerical simulations of Eqs. (3) we have integrated them by different numerical methods: an alternating direction implicit method, a Crank-Nicholson's method, and a split-step method with pseudospectral integration of the spatial derivatives [17], all of which lead to identical results. The

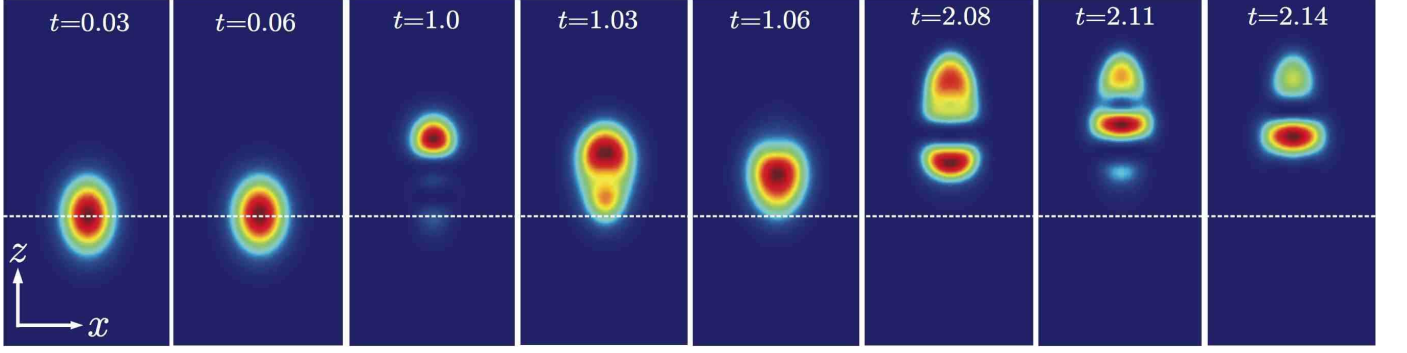


FIG. 4: Pseudocolor plots of $|\psi_2(x, z, t)|^2$ on the region $(x, z) \in [-6.5, 6.5] \times [-7.1, 6]$ for different values of t and $\delta z = 5.0$, $B' = 50$. The time spacing between all panels, except for panels 2 and 3 and panels 5 and 6, is half the Rabi period τ_{RB} .

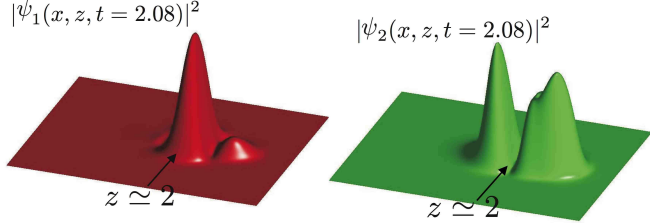


FIG. 5: Surface plots of $|\psi_1(x, z, t = 2.08)|^2$ (red) and $|\psi_2(x, z, t = 2.08)|^2$ (green) for the situation described in Fig. 4. The arrow indicates the location of maximum density of $|\psi_1|^2$ corresponding to a low-density region of $|\psi_2|^2$. The spatial region shown in the plot is $(x, z) \in [-6.5, 6.5] \times [-6.5, 6.5]$

values of the scaled parameters used throughout the text are: $U'_{11} = 100$, $U'_{22} = 97$, $U'_{12} = 94$; $g' = 0.1$; $z_1^* = -2.5$ and $z_2^* = -z_1^*$ with $\delta z = z_2^* - z_1^* = 1, 3$ and 5 . $\epsilon'_1 = -250$, $\epsilon'_2 = 250$ and $\delta\epsilon' = \epsilon'_2 - \epsilon'_1 = 500$ [18].

First we study the population mixing between the components. In the standard resonance case ($\Omega' = \delta\epsilon' = \epsilon'_2 - \epsilon'_1$) without coupling with the orbital degrees of freedom, the Rabi formula implies that each $P_j(t) (= \int |\psi_j|^2 d^2\mathbf{r})$ shows a fast oscillation whose frequency is proportional to the magnetic field amplitude B' [19]. In our Franck-Condon type transition ($\Omega' = \Delta V'_{12}$), the spatial orbital functions of BEC are coupled with the electronic degrees of freedom, and the Rabi oscillation (with period $\tau_{RB} = 2\pi/B'$) becomes modulated sooner or later. In Fig. 2 we show the time dependence of both populations for different values of the distance between trap centers δz . We find that unless δz is sufficiently small, the regular oscillation responsible for population mixing becomes suppressed as time elapses, which is attributed to the energy conversion from electronic to mechanical energy.

We have also studied the motion of the total center of mass (CM) of the system along the vertical direction defined by $\bar{z} = \int \psi^\dagger z \psi d^2\mathbf{r} = \int z (|\psi_1|^2 + |\psi_2|^2) d^2\mathbf{r}$.

In Fig. 3(a), except for the lowest curve, we show typical examples of the time evolution of the center of mass. In the Franck-Condon resonance situation de-

scribed above we find a rising of the total center of mass against gravity. This is an interesting phenomenon which happens while the underlying population mixing shows a fast Rabi oscillation. In our numerical simulations we observe that the CM of the condensate exhibits a smooth and upward acceleration, reaching a maximum height $\sim z_2^*$ for $t = 2.2$ corresponding to $(2.2/\tau_{RB} \sim 18$ Rabi periods) for $B' = 50$. This physical phenomenon is a *levitation of the condensate through a macroscopic quantum transition which is not accompanied by neither an applied mechanical force nor a classical trajectory*. Figs. 3(b) and (c) are the total probability density $|\Psi(x, z, t)|^2 = |\psi_1(x, z, t)|^2 + |\psi_2(x, z, t)|^2$ before and after the levitation, respectively. The levitation effect becomes more pronounced as δz is increased. It is very interesting to point out that no levitation occurs in the case far from the standard resonance ($\Omega' \ll \delta\epsilon'$), which is confirmed in the lowest curve in Fig. 3(a).

Fig. 4 shows the spatiotemporal dynamics of the wavefunction $|\psi_2(x, z, t)|^2$ for times located in the three regions which are clearly discriminated in the dynamics for $\delta z = 5$. First, in the early stage region ($t = 0 \sim 0.5$) the wavefunction oscillates near the minimum (z_1^*) of the lower potential well. As time goes on ($t = 1 \sim 1.5$), the central position of the solutions moves towards the minimum of the upper well (z_2^*). Finally, when the CM position reaches its peak value $\sim z_2^*$ for $t = 2 \sim 2.2$, the wavefunction has a double-humped structure with its valley located near the minimum of the upper well. Fig. 5 shows that the two components $|\psi_{1,2}|^2$ form a domain structure in this time region, a typical feature of the system due to the nonlinear interactions. The nonlinearity plays an important role in the formation of domain structures during the transitions, a feature which is not present in the noninteracting case.

The origin of this transport phenomenon is that the condensate is effectively driven by the oscillating magnetic field to the higher energy states of the upper level, thus leading to a Franck-Condon type vertical transition. After the transition the new position is unstable, and the

atoms relax towards the new minimum (at the position with larger z), leading to the observed transport.

We have studied the dependence of the levitation phenomenon on the problem parameters B' and $\delta z = z_2^* - z_1^*$. In Fig. 6(a) we show the dependence on B' of the upward acceleration rate, α , evaluated by using a quadratic function of t ($\bar{z} = z_1^* + \frac{1}{2}\alpha t^2$) which is fitted to the CM data in the early stage region. Interestingly, α has a maximum at some optimal value of B' . This fact indicates that the Rabi oscillation is essential for the energy conversion between electronic and orbital degrees of freedom; however, when the Rabi oscillation is too fast to guarantee the relaxation towards z_2^* , there is a reduction of the effective energy conversion.

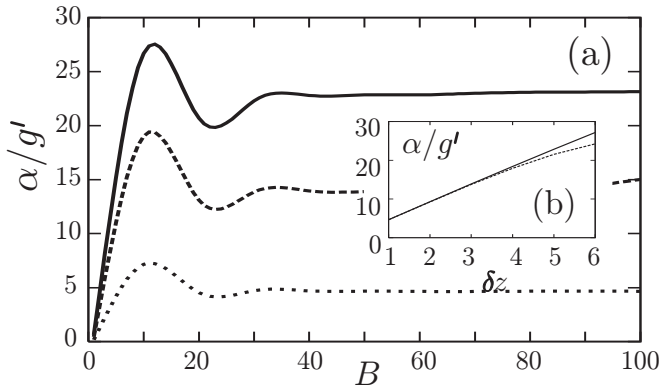


FIG. 6: Upward acceleration rate (α) for the motion of the center of mass during the levitation process (a) B' dependence in the cases $\delta z = 1$ (dotted line), $\delta z = 3$ (dashed line), $\delta z = 5$ (solid line); (b) Dependence of α on δz for $B' = 50$ the Franck-Condon (solid line) and standard (dotted line) resonances.

In Fig. 6(b) we see that under a fixed B' , α increases monotonically in δz , but indicates a slight derivation from the linear law in the case of non-Franck-Condon type transition (e. g. in the case of standard resonance, $\Omega' = \delta\epsilon'$).

In conclusion, we have studied the dynamics of two-component Bose-Einstein condensates subject to an a.c. driving magnetic field. In the case of Franck-Condon's vertical transition in which the driving frequency Ω corresponds to the energy difference between the trapping potentials V_1 and V_2 at the minimum position z_1^* of V_1 , the condensate initially located around z_1^* is effectively driven to unstable states of V_2 , relaxing towards the potential minimum z_2^* ($= z_1^* + \delta z$) of V_2 . In this situation the population mixing shows a fast Rabi oscillation, while the mean center-of-mass of the condensate exhibits a smooth and upward acceleration with its rate (α) showing a maximum at some optimal magnetic-field amplitude and a monotonic increase in δz . This phenomenon is a manifestation of macroscopic non-adiabatic quantum tunneling with internal degrees of freedom, which differs essentially from other quantum tunneling processes with Bose-Einstein condensates discussed up to now.

This work has been partially supported by grants BFM2003-02832 (Ministerio de Educación y Ciencia, Spain) and PAI-05-001 (Consejería de Educación y Ciencia de la Junta de Comunidades de Castilla-La Mancha, Spain).

* Electronic address: nakamura@a-phys.eng.osaka-cu.ac.jp
† Electronic address: victor.perezgarcia@uclm.es

- [1] M. H. Anderson, *et al.*, *Science* **269**, 198 (1995); K. B. Davis, *et al.*, *Phys. Rev. Lett.* **75**, 3969 (1995); C. C. Bradley, C. A. Sackett, and R. G. Hulet, *Phys. Rev. Lett.* **78**, 985 (1997).
- [2] D. Hall, *et al.*, *Phys. Rev. Lett.* **81**, 1539 (1998).
- [3] D. Hall, *et al.*, *Phys. Rev. Lett.* **81**, 1543 (1998).
- [4] M. R. Matthews *et al.*, *Phys. Rev. Lett.* **81**, 243 (1998).
- [5] J. Stenger, *et al.*, *Nature (London)* **396**, 345 (1998); H.-J. Miesner, *et al.*, *Phys. Rev. Lett.* **82**, 2228 (1999).
- [6] M. R. Matthews, *et al.*, *Phys. Rev. Lett.* **83**, 2498 (1999).
- [7] J. Williams, *et al.*, *Phys. Rev. A* **59**, R31 (1999); M. R. Matthews, *et al.*, *Phys. Rev. Lett.* **83**, 3358 (1999).
- [8] J. J. García-Ripoll, V. M. Pérez-García, F. Sols, *Phys. Rev. A* **66**, 021602(R) (2002).
- [9] B. Wu and Q. Niu, *Phys. Rev. A* **61**, 023402 (2000); O. Zobay and B. M. Garraway, *Phys. Rev. A* **61**, 033603 (2000); J. Liu, B. Wu, Q. Niu, *Phys. Rev. Lett.* **90**, 170404 (2003); E. A. Ostrovskaya and Y. S. Kivshar, *Phys. Rev. Lett.* **92**, 180405 (2004).
- [10] M. Cristiani, *et al.*, *Phys. Rev. A* **65**, 063612 (2002); A. Smerzi, *et al.*, *Phys. Rev. Lett.* **79**, 4950 (1997).
- [11] M. D. Barrett, J. Sauer and M. S. Chapman, *Phys. Rev. Lett.* **87**, 010404 (2001); Y. Shin, *et al.*, *Phys. Rev. Lett.* **92**, 150401 (2004); M. S. Chang, *et al.*, *Phys. Rev. Lett.* **92**, 140403 (2004).
- [12] B. Deconinck, P. G. Kevrekidis, H. E. Nistazakis, D. J. Frantzeskakis, *Phys. Rev. A* **70**, 063605 (2004); P. G. Kevrekidis, *et al.*, *Phys. Rev. E* **72**, 066604 (2005).
- [13] M. Albiez, *et al.*, *Phys. Rev. Lett.* **95**, 010402 (2005); R. Gati, *et al.*, *Phys. Rev. Lett.* **96**, 130404 (2006).
- [14] L. D. Landau and E. M. Lifshitz, *Quantum Mechanics* (Pergamon, Oxford, 1958).
- [15] J. Franck, *Trans. Faraday Soc.* **21**, 536 (1925); E. U. Condon, *Phys. Rev.* **28**, 1182 (1926); *ibid* **32**, 858 (1928).
- [16] V. M. Pérez-García, H. Michinel, H. Herrero, *Phys. Rev. A* **57**, 3837 (1998).
- [17] See, e. g., S. K. Adhikari, *Phys. Rev. E* **63**, 056704 (2001); V. M. Pérez-García, X. Liu, *Appl. Math. Comput.* **144** (2003) 215.
- [18] Although ϵ_j' is of the order of GHz/Hz our results should be valid for any $\delta\epsilon'$, provided $\delta\epsilon' \gg 1$ as it happens for Franck-Condon or standard resonances. This is so because in the rotating-wave approximation (RWA), the unitary transformation of wave functions that makes static the oscillating field produces in the diagonal term the difference between Ω' and $\delta\epsilon'$. This difference is much less than unity in the case of Franck-Condon resonance and vanishes in the case of standard resonance. Since we are not working in the RWA, we use the oscillating field as it stands and choose a large enough value of $\delta\epsilon' = 500$.
- [19] J. J. Sakurai, *Modern Quantum Mechanics* (Addison Wesley, New York, 1994).